



# Site-specific deterministic and probabilistic tsunami hazard assessment for Diba-Oman and Diba-Al-Emirates

Issa El-Hussain<sup>1</sup> · Zaid Al-Habsi<sup>1</sup> · Khalid Al Bloushi<sup>2</sup> · Rachid Omira<sup>3,4</sup> · Ahmed Deif<sup>1</sup> · Maria Ana Baptista<sup>3,4,5</sup> · Adel M. E. Mohamad<sup>1,6</sup>

Received: 8 October 2020 / Accepted: 22 April 2021 / Published online: 6 May 2021  
© Saudi Society for Geosciences 2021

## Abstract

Destructive tsunamis were reported in the Oman Sea after large earthquakes. The Northern Sultanate of Oman and United Arab Emirates (UAE) were subjected to two confirmed tsunamis on 27 November 1945, caused by an Mw 8.1 earthquake in Makran subduction zone, and on 24 September 2013 following the Mw 7.7 Baluchistan earthquake. In this study, deterministic and probabilistic tsunami hazard assessments are performed for the coasts of Diba-Oman and Diba-UAE, which are located on the western coast of the Oman Sea. The tsunami risk of these coasts increases due to the construction of many infrastructures and urban concentration in these localities. The study focuses on earthquake-induced tsunamis, thus requiring the estimation of the maximum credible earthquake. The generation area is the Makran subduction zone, which is divided herein into EMSZ (East Makran subduction zone) and WMSZ (West Makran subduction zone). The maximum credible earthquakes of Mw 8.8 for the EMSZ and Mw 7.2 for the WMSZ are utilized as specific scenarios for the deterministic approach. The Mw 8.8 EMSZ scenario results in a maximum tsunami inundation distance of more than 300 m. Maximum inundation distance larger than 300 m occurs due to the Mw 7.2 western MSZ scenario. For these scenarios, numerical simulations show a maximum flow depth exceeding 1.75 m. The probabilistic hazard assessment utilizes the logic tree approach to estimate the probability of exceedance of 0.25, 0.5, 0.75, and 1.0 m wave height in 100 and 500 years exposure times. This analysis indicates that the likelihood that a maximum wave height exceeds 0.5 m ranges from 10 to 40% in 100 years and from 30 to 80% in 500 years.

**Keywords** Diba · Makran subduction zone · Deterministic tsunami · Probabilistic tsunami

This article is part of the Topical Collection on *Seismic and Earthquake Engineering Studies in the Arabian Plate and the Surrounding Region*.

Responsible Editor: Longjun Dong

✉ Issa El-Hussain  
elhussain@squ.edu.om

<sup>1</sup> Earthquake Monitoring Center, Sultan Qaboos University, P.O. Box 50, Al-Khoudh, PC 123 Muscat, Oman

<sup>2</sup> Department of Earth Science, United Arab Emirates University, Al Ain, United Arab Emirates

<sup>3</sup> Instituto Dom Luiz, University of Lisbon, IDL-FCUL, Lisbon, Portugal

<sup>4</sup> Instituto Português do Mar e da Atmosfera, Rua C do Aeroporto, 1749-077 Lisbon, Portugal

<sup>5</sup> Instituto Superior de Engenharia de Lisboa, Instituto Politécnico de Lisboa, R. Conselheiro Emídio Navarro, 1, 1959-007 Lisboa, Portugal

<sup>6</sup> National Research Institute of Astronomy and Geophysics, Helwan, Cairo, Egypt

## Introduction

Throughout history, severe tsunamis were responsible for considerable loss of life and property worldwide. The major cause of tsunamis is large submarine earthquakes, but landslides (submarine and aerial), volcanic eruptions, atmospheric disturbances, meteorite impacts, and snow avalanches also account for tsunami sources. Tsunamis of tectonic origin can cause ocean-wide impact because their induced waves can travel far away from the source without much energy dissipation. The 26 December 2004 tsunami is a recent example of ocean-wide devastating events that affected 12 countries of the Indian Ocean and caused over 230,000 fatalities (Titov et al. 2005).

Oman and United Arab Emirates (UAE) are among the Indian Ocean countries that are exposed to tsunami threat from regional and distant large earthquakes occurring within active subduction zones. The Makran subduction zone (MSZ), in the Sea of Oman (Fig. 1), is probably the major known source of tsunamis to impact both coasts of Oman and

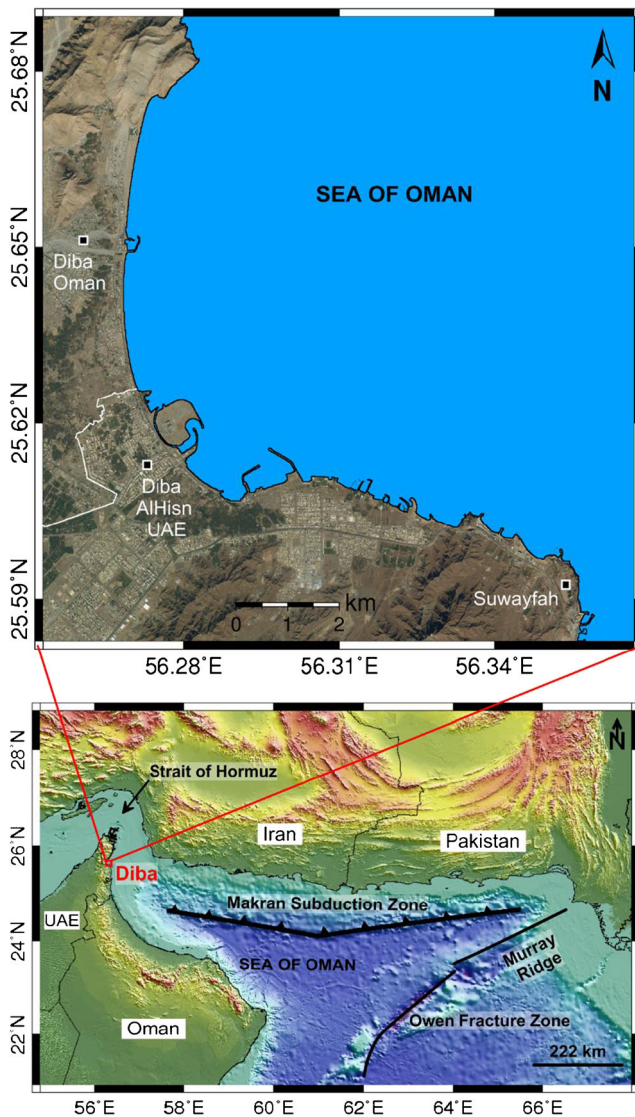


**Fig. 1** Map showing the Diba-Oman and Diba-Al-Emirates coastal areas along the Sea of Oman

UAE, posing a real threat on their coastal communities. Here, the 27 November 1945 Oman Sea tsunami, caused by an Mw 8.1 earthquake off Makran coast of Pakistan, considerably damaged the coasts Pakistan, India, and Iran, whereas lesser tsunami impact was reported on the coast of Oman. Oman may also be affected by far field tsunamis generated within the Andaman Sumatra subduction zone (ASSZ) in the Indian Ocean. This subduction zone was responsible for the megathrust Mw 9.1 earthquake on 26 December 2004 that caused a devastating transoceanic tsunami but with minor damage reported in the southern coast of Oman (Okal et al. 2006). Despite the recognized threat posed by tsunamis of tectonic origin on the coasts of Oman and UAE, quantitative hazard assessments, involving high-resolution estimates of tsunami metrics, are still lacking for most coastal sectors. In this study, we target the 30-km-long coast hosting Diba-Oman and Diba-UAE (Fig. 1) to conduct quantitative tsunami hazard

assessment. Diba-Oman and Diba-UAE are located on the west coast of Oman Sea, south of an important water entrance passage named the Strait of Hormuz (Fig. 1). While Diba-Oman is a small coastal town with 5000 inhabitants and a large natural harbor on the west coast of the Sea of Oman, Diba-UAE is one of the largest towns in Al-Fujairah (one of the seven emirates of the UAE) that contains several small villages located between the mountains and the coast. Both are young cities with active and ambitious development plans of commercial ports, fishing ports, and leisure ports necessitating tsunami hazard assessment for preparation and implementation of mitigation measures.

This study evaluates the tsunami hazard on Diba-Oman and Diba-UAE coasts using both deterministic and probabilistic approaches. Tsunami hazard along the coast of Diba-Oman and Diba-UAE is mainly due to the seismic activity at the MSZ located circa 150 to 600 km towards east. Here, the tsunamigenic source region that has the potential to affect the study area is delineated based on historical earthquake records, tsunami data, and sea bathymetric data. For the deterministic method, the source mechanism and characteristics of the worst-case scenarios are evaluated based on the maximum magnitude earthquake estimated by El-Hussain et al. (2016) and Deif et al. (2020). The established source parameters are then used to numerically model the tsunami caused by the worst-case scenarios and to derive the potential inundation and runup heights maps.

## Tsunamigenic potential in the Oman Sea

Countries in the Sea of Oman, including Oman and UAE, are threatened by tsunamis from two major seismogenic sources in the Indian Ocean. These are the MSZ as the near field tsunami source and the ASSZ as a far field tsunami source. A survey of the tsunami history in the region indicates that at least one confirmed tsunami from the MSZ struck the coasts of Oman Sea in 1945 due to the great earthquake with moment magnitude 8.1 occurred off Makran coast of Pakistan, about 100 km south of Karachi (Rashidi et al. 2020a, b). The earthquake generated a very destructive tsunami, which is reported to affect Pakistan, the western coast of India, Iran, UAE, and Oman, killing hundreds of people and causing great destruction. A maximum runup height of 13 m is reported in Pakistan (Pendse 1946; Mokhtari et al. 2008). The tsunami was observed in Muscat, but no details of damage were documented. Another minor tsunami was recorded in several tide stations along the northeast coast of Oman following the 24 September 2013 Baluchistan earthquake of magnitude 7.7 in Pakistan 100 km north of Makran coast (Baptista et al. 2014, 2020). From the ASSZ, the Indian Ocean 2004 horrific tsunami reached the eastern coasts of the Oman affecting the southern part of the coast (Okal et al. 2006). This fact suggests that the

primary tsunami threat to study area (Diba-Oman and Diba-UAE) is from the MSZ as the far field from the ASSZ generates modest tsunamis along this part of the coast.

The tectonic of the Oman Sea is constrained by the relative motion between the Arabian, Eurasian, and India plates (Fig. 2). The Arabian Plate subducts under the Eurasian Plate at a rate close to 2 cm/year. The relative motion between India and Arabian Plates along the Owen strike slip boundary reaches 3.7 mm/year (Vernant et al. 2004). The MSZ is more than 800 km long north dipping thrust tectonic feature, where this part of the Arabian Plate subducts beneath the Iranian and Pakistani segments of the Eurasian Plate (Fig. 2a). Its low seismicity shows significant variation between its eastern and western segments. The large variation in seismic activities between the eastern and western parts of MSZ, along with the rupture history variations (Minshull et al. 1992; Musson 2009) and other geological observations, led to the belief that the eastern part is completely separate from the Western Makran. This explains why most of the seismic activity occurs in the eastern part of the zone, and the western part is apparently quiet. The eastern Makran (see Fig. 2b) has been ruptured by large earthquakes and is the location of the 28 November 1945 large earthquake of 8.1 magnitude (El-Hussain et al. 2017). This segment is still active but experiencing low seismic activity at present time. The lack of large tectonic earthquakes in Western Makran implies either that aseismic subduction takes place or that the plate boundary

is currently locked and great earthquakes with long repeat times are expected. Bayer et al. (2006) argued that the absence of large earthquakes in the Western Makran can be explained by the fact that this area is marked by a great amount of unconsolidated and water saturated deposits, which may result in a low frictional coefficient, as the weak sediments lubricate relative plate movement so as to constrain seismicity. Thus, the subduction could be near aseismic. Additionally, George Pararas-Carayannis (2006) indicated that the western segment of MSZ shows much more fracturing, indicating that earthquakes would be expected to be smaller-magnitude events (< 7) and to have shorter ruptures (< 100 km) along sub-segments (in coincident with the scenarios of the current study).

## Methods and model setup

### Deterministic and probabilistic tsunami hazard assessment

Existing tsunami hazard assessment methods include the deterministic tsunami hazard assessment (DTHA) and the probabilistic tsunami hazard assessment (PTHA). The DTHA employs particular source scenarios (i.e., maximum credible or worst-case scenario) to numerically predict and map selected hazard metrics (e.g., maximum wave height, flow depth,

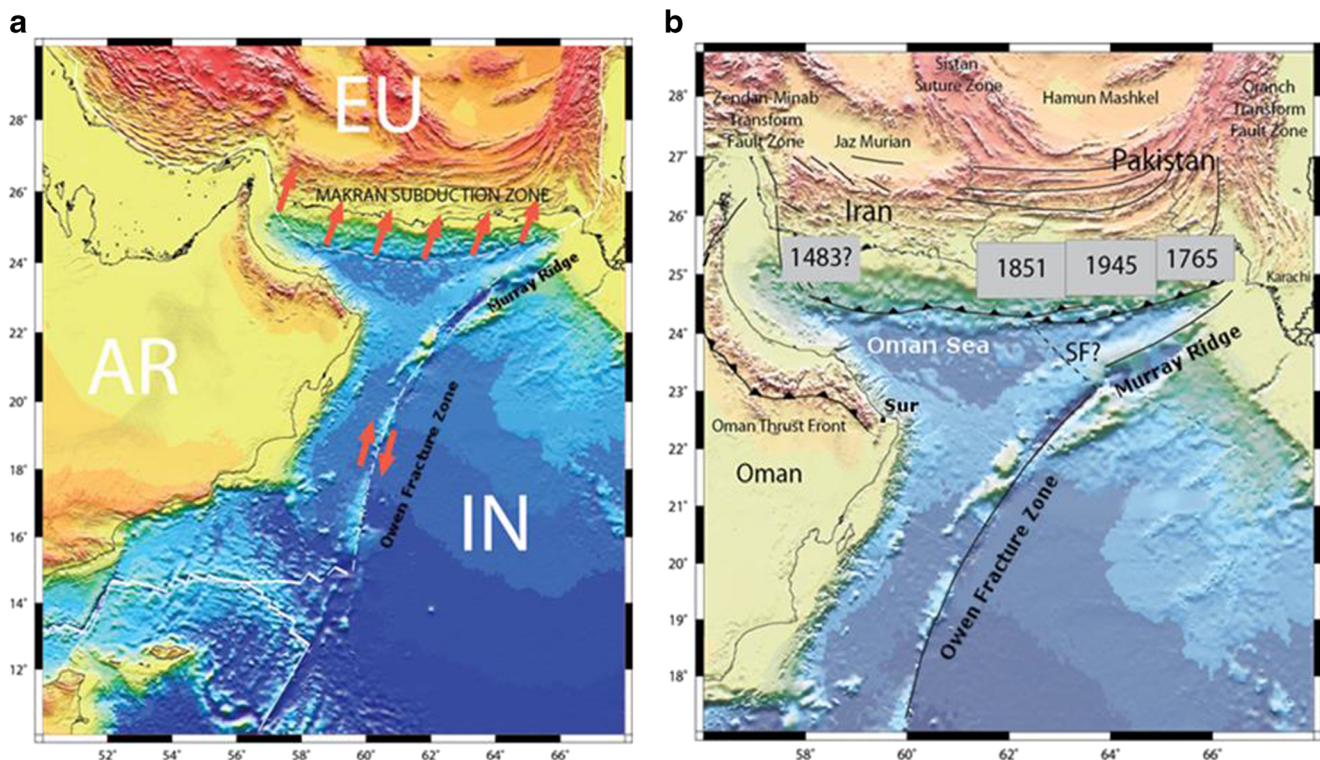


**Fig. 2** a The tectonic of the Sea of Oman showing the relative motion between the Arabian, Eurasian, and India plates. b Ruptured area of strong earthquakes in Makran based on Byrne et al. (1992) and Zarifi

(2006). AR Arabian Plate, IN Indian Plate, EU Eurasian Plate, SF Sonne Fault, defining a small microplate, called Ormara microplate by Kukowski et al. (2000)

current velocity). The PTHA, on the other hand, determines the likelihood of exceeding a specific tsunami hazard intensity (e.g., wave height, runup height) at a particular location within a given time period by integrating the modeled hazard from all possible events (Geist and Parsons 2006; Grezio et al. 2017). Although the DTHA is considered simple to conduct and provides easily interpreted results, it is very sensitive to the selection of the source scenario (Geist and Lynett 2014). In comparison to the DTHA, PTHA is relatively complex and computationally demanding. The complexity of the PTHA relies on the treatment of uncertainties that often leads to generate a large number of possible events.

In the DTHA, the earthquake scenarios able to cause the worst tsunami impact on Diba-Oman and Diba-UAE coasts are defined. Based on available seismic information, the definition of the tsunamigenic scenarios consists of determining the earthquake fault parameters necessary to simulate the ensuing tsunami and then numerically modeled the tsunami generation and propagation towards the target coast. Finally, the DTHA results are presented for each individual scenario in terms of tsunami travel time, maximum wave heights, and inundation maps.

In the PTHA, the event-tree developed by Omira et al. (2016a) and applied for the coast of Oman in El-Hussain et al. (2016) and El-Hussain et al. (2018) is used. The event-tree incorporates the following nodes: (i) tsunamigenic source zones definition within the MSZ; (ii) database of the earthquake scenario generated within each source zone; (iii) determination of the earthquake recurrence rate; (iv) simulation of the tsunami, associated to each defined scenario, from the source to the target coast; and (v) deriving the tsunami probability of exceedance using statistical methods. The PTHA results are presented as hazard maps expressing the probability of exceeding maximum wave heights/flow depths of 0.05, 0.25, 0.5, and 1.0 m for exposure times of 100 and 500 years.

## Model setup

### Tsunami scenarios

For the DTHA, the source mechanism and characteristics of the worst-case scenarios are evaluated based on the

**Fig. 3** DEM showing bathymetry and topography grid with four nested grid levels used for Diba tsunami simulation with grid spacing of 1250m, 250m, 50m, and 10m, respectively

maximum magnitude earthquake estimated by El-Hussain et al. (2016) and Deif et al. (2020) and on the available historical earthquake records, tsunami data, and sea bathymetric data. Two maximum credible earthquakes of Mw 8.8 for the east and Mw 7.2 for the west MSZ, with several hundred years catalog duration and active tectonic elements in the region (Deif and El Hussain 2012; El-Hussain et al. 2018), are considered the worst-case tsunami scenarios for the study area. Additionally, the tsunami impact from the Mw 8.1 earthquake scenario representing the historical 1945 event is also determined. Table 1 summarizes the earthquake fault parameters for the considered tsunamigenic scenarios.

For the PTHA, we generate a database of 400 earthquake scenarios able to cause tsunamis that reach/impact the study coasts of Diba-Oman and Diba-UAE. The PTHA scenario database includes earthquake magnitudes ranging from Mw 6.5 to Mw 8.8, with a regular interval of 0.1 between individual magnitudes. The minimum and maximum earthquake magnitudes are, respectively, set to Mw 6.5 and Mw 8.8 for the eastern MSZ and to Mw 6.5 and Mw 7.2 for the western MSZ. The recurrence rate of each individual magnitude is calculated using two different seismic probability models, Molnar (1979) and Deif and El Hussain (2012), based on moment rate. For each individual magnitude, we associate a typical fault that we let float along the fault trace to cover the uncertainty on the earthquake location (Omira et al. 2015, 2016a; El-Hussain et al. 2016, 2018).

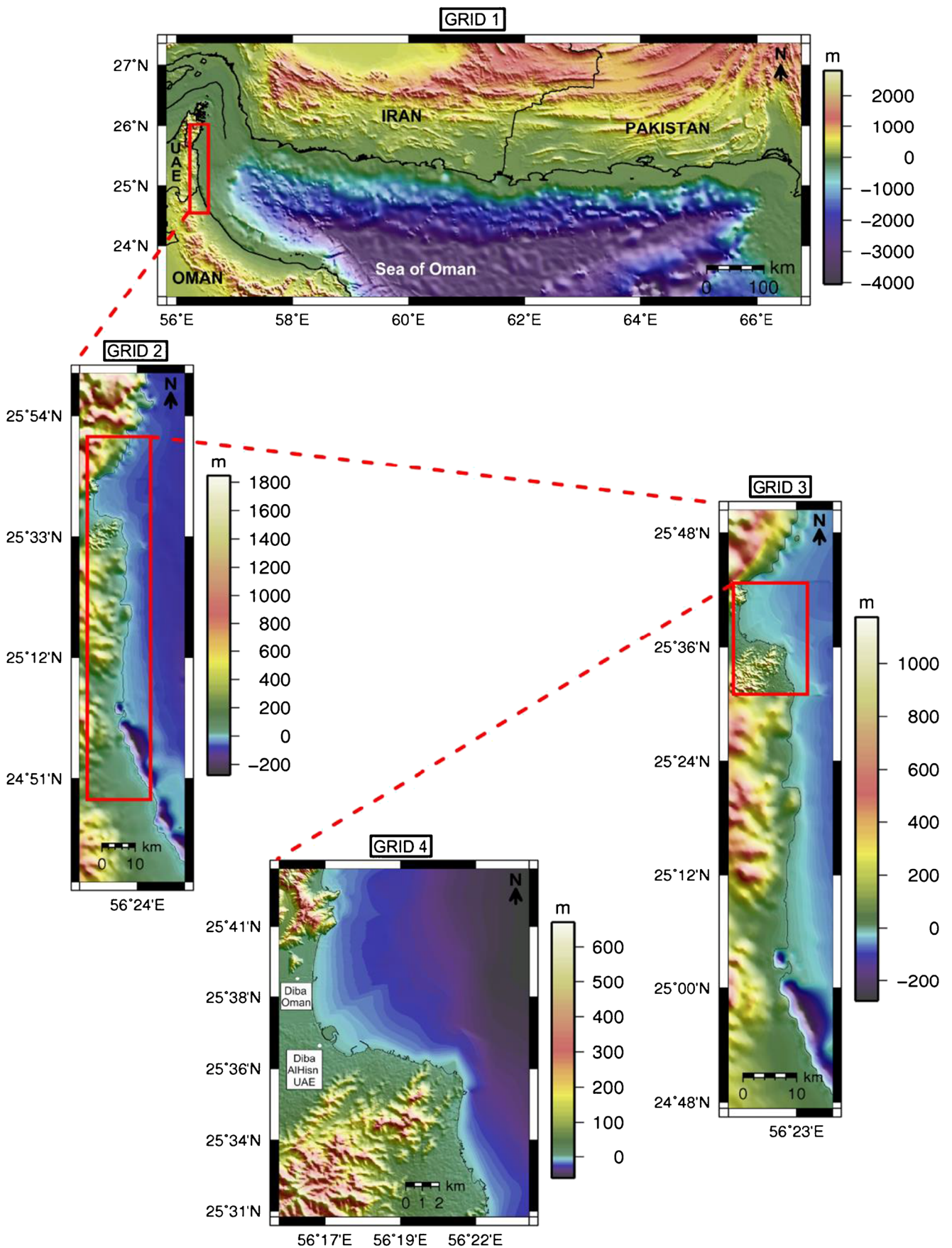
### Digital elevation models

Tsunami numerical simulation needs high-quality digital elevation model (DEM). The DEM is a major controlling factor in tsunami simulation. Figure 3 shows the DEM used here and the computational grids. Four nested grids with a refinement factor of five were used, with the grid resolution varying from 1250 m in the source region to 10 m in the Diba area. For deep ocean tsunami simulation,

**Table 1** Makran subduction zone tsunamigenic earthquake scenarios

Scenario	Mw	Location <sup>a</sup>		Length ( km)	Width (km)	Slip (m)	Dip ( °)	Rake ( °)	Strike ( °)
		Latitude (°N)	Longitude (°E)						
WMSZ	7.2	24.53	58.21	62	25	1.7	7	90	281
EMSZ	8.8	24.66	65.50	461	110	11	7	90	263
HMSZ	8.1	25.17	64.98	150	70	6.6	7	90	246

<sup>a</sup> The southeast corner of the fault plane



GEBCO 15 second arc resolution gridded data were used to prepare the outermost grids. Digitization of local bathymetry map obtained from the Omani National Survey Authority (NSA) was performed to generate a near-shore bathymetry with 30m resolution. The fusion of high-resolution depth and height data requires a common definition for the vertical reference surface. The zero-elevation contour line was created from digitizing the shoreline using Google Earth Pro and is used as the boundary for land-sea transition. For the innermost grid, a local topography data of 5 m resolution obtained from NSA and 30 m resolution NASA Shuttle Radar Topography Mission (SRTM) was combined with the local bathymetry and GEBCO data to produce a uniform bathymetric and topographic dataset with a spatial resolution of 10 m through interpolation. Data gaps between the bathymetry and topography were interpolated and completed up with data from nautical charts. All combined datasets were transformed to the same reference system considering that the vertical datum is the Mean Sea Level (MSL) and WGS84 geographic coordinate system map projection.

### Tsunami numerical model and PTHA framework

Numerical simulations are performed for tsunami generation, propagation, and coastal inundation for both DTHA and PTHA scenarios. The formation of the tsunami is computed using the half-space elastic theory (Okada 1985) and assuming that the earthquake rupture is supposed instantaneous and the vertical sea bottom displacement mimics the free ocean surface deformation. Simulations of tsunami propagation and inundation are conducted over the nested grid system developed for this study (Fig. 3) and using the benchmarked numerical code NSWING (non-linear shallow water model with nested grids) (Miranda et al. 2014). NSWING code solves shallow water equations using an explicit staggered leap-frog finite differences numerical scheme for linear terms and an upwind scheme for the non-linear terms. NSWING was used to simulate the tsunami in various regions of the globe (Omira et al. 2016b; Baptista et al. 2017).

The PTHA framework allowing to establish, the multi-source joint probability that a tsunami metric (wave height/flow depth) exceeds a threshold at a given exposure time, considers the sources as independent (as in the Poisson distribution). This process enables calculating the time-independent probability that tsunami hazard intensity will be exceeded following an earthquake scenario (Omira et al. 2015, 2016a). Previous works (Omira et al. 2015, 2016a; El-Hussain et al. 2016) provide a detailed description of the PTHA framework used here.

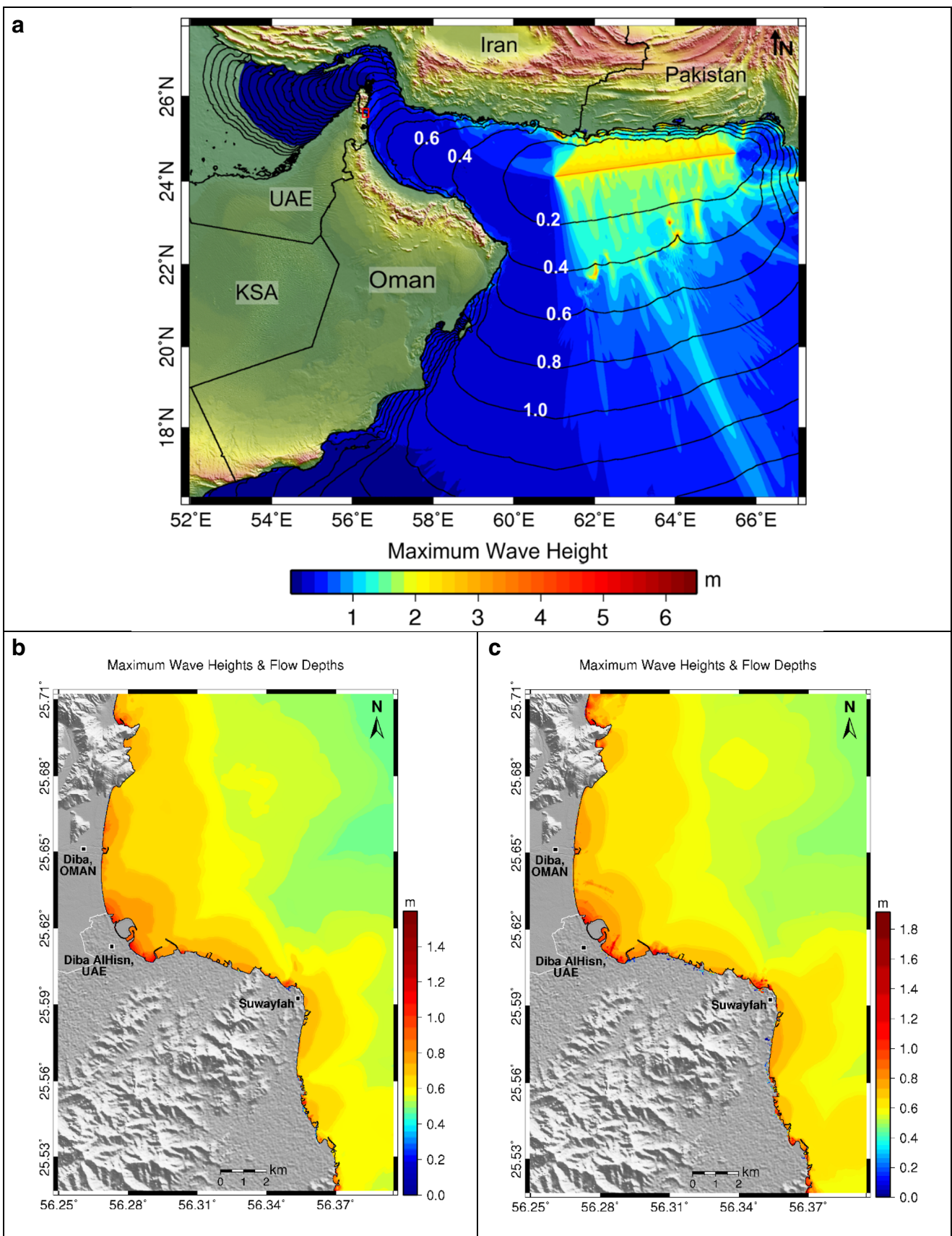
## Results

### Deterministic tsunami hazard

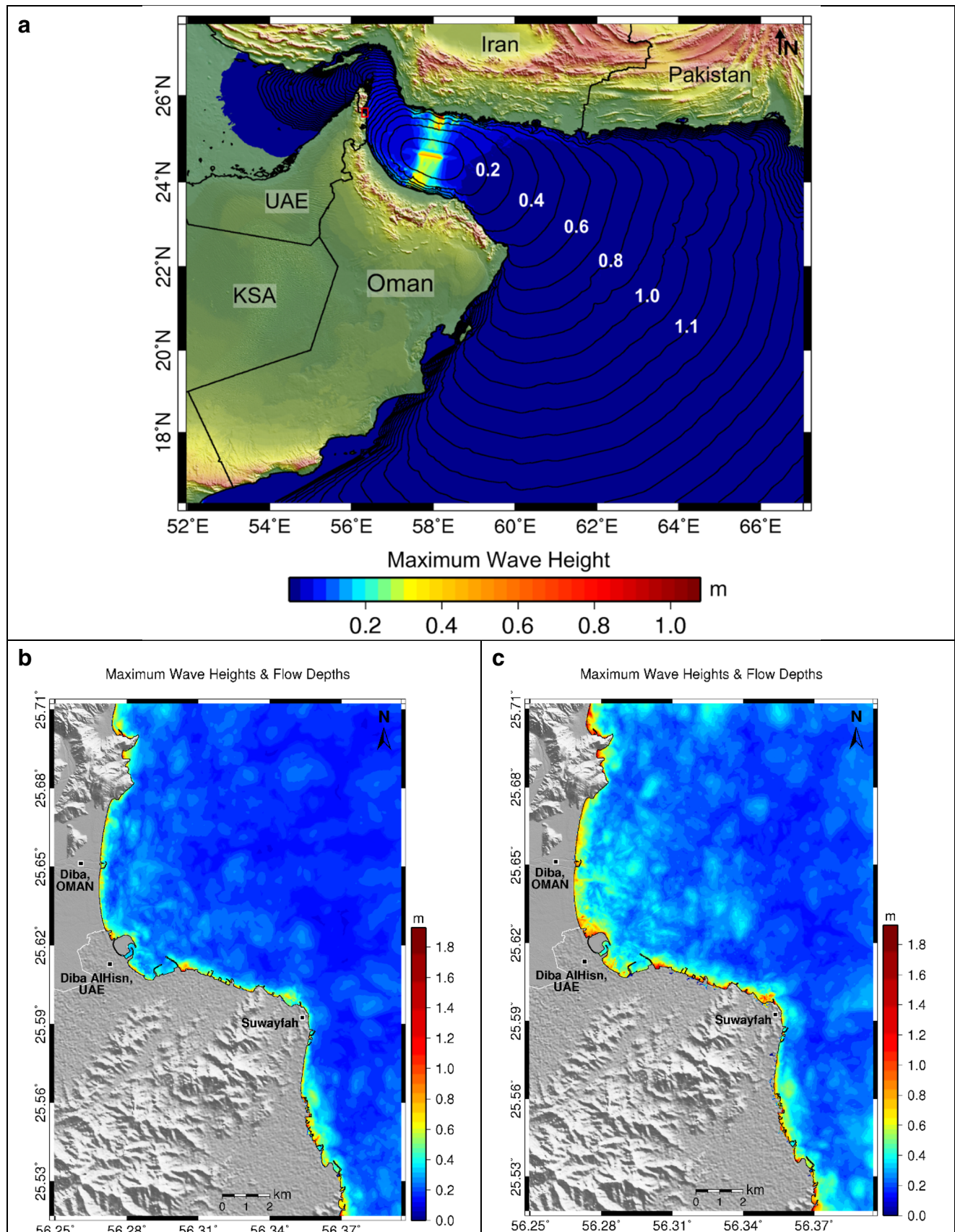
Numerical simulations of the tsunami propagation from the source area to the target coast with onshore propagation (inundation) are conducted. Here, the mean high-high water (MHHW) was considered in the simulation so that 0.81m was added to the DEM for DTHA simulations. The outputs of this assessment are maps of tsunami travel time (Fig. 4a), maximum wave height and flow depths and inundation distances (Fig. 4b and c). Both wave height and flow depth refer to the sea surface elevation offshore above the mean sea level and inland above the ground level, respectively. Inundation distance presents the inland tsunami penetration horizontal distance calculated between the coastline and the flood limit. Figure 4a depicts contours representing the tsunami travel times (TTT) in hours, estimated using bathymetric coarse grid of 30 s arc resolution, arriving at Diba coasts in 84 minutes following the occurrence of Mw 8.8 earthquake event in Eastern MSZ. Figure 4b and c are the tsunami hazard maps showing the maximum inundation distances of 220 and 305 m and the maximum flow depths of 1.50 and 1.90 m for Diba area when tsunami occurs during mean sea level and MHHW, respectively, due to the Mw 8.8 scenario from Eastern MSZ. Runup heights, vertical heights above the sea level of the onshore point reached by the tsunami, are obtained as 1.20 and 2.80 m during mean sea level and MHHW, respectively, when crossing the inundation limits with the coastal topography. The TTT to Diba coast is about 45 min following the occurrence of Mw 7.2 in West MSZ scenario (Fig. 5a). The west MSZ scenario generates 128 and 305m inundation distances, 1.6 and 1.8m flow depths, and 1.25 and 2.3 m runup heights in Diba area when the tsunami occurs during mean sea level and MHHW, respectively (Fig. 5b and c).

Figure 6a is a regional map showing maximum wave height and a TTT of 108 min arriving to Diba coasts following the occurrence of historic Mw 8.1 earthquake event in 1945 in Eastern MSZ. Figure 6b is the tsunami hazard map showing the maximum inundation distance of 70 m, the maximum flow depth of 0.4m, and allowing to extract a runup height of 0.2 m for Diba coasts, due to the Mw 8.1 historic earthquake in Eastern MSZ.

Figure 7 shows the inundation area for the worst-case scenarios for EMSZ and WMSZ for MHHW conditions. We notice that for both scenarios, the obtained tsunami inundation area is comparable as flood limits (red and blue contours in Fig. 7) almost coincide. The green circles show the worship places, and pink squares the schools in the area. For the scenarios studied here, it appears that most of these structures are out of the inundation zone. Nevertheless, in the event of an offshore earthquake of magnitude greater than 7, evacuations and preparedness plans are still needed for these coastal cities.



**Fig. 4** a Tsunami travel time in hours for scenario Mw 8.8, eastern MSZ, **b** and **c** are tsunami hazard map for Diba representing maximum wave height/ flow depth and inundation in meters during mean sea levels and MHHW respectively, for scenario  $M_w$  8.8



**Fig. 5** **a** Tsunami travel time in hours for scenario Mw 7.2, western MSZ, **b** and **c** are tsunami hazard map for Diba representing maximum wave height/flow depth and inundation in meters during mean sea levels and MHHW respectively, for scenario Mw 7.2



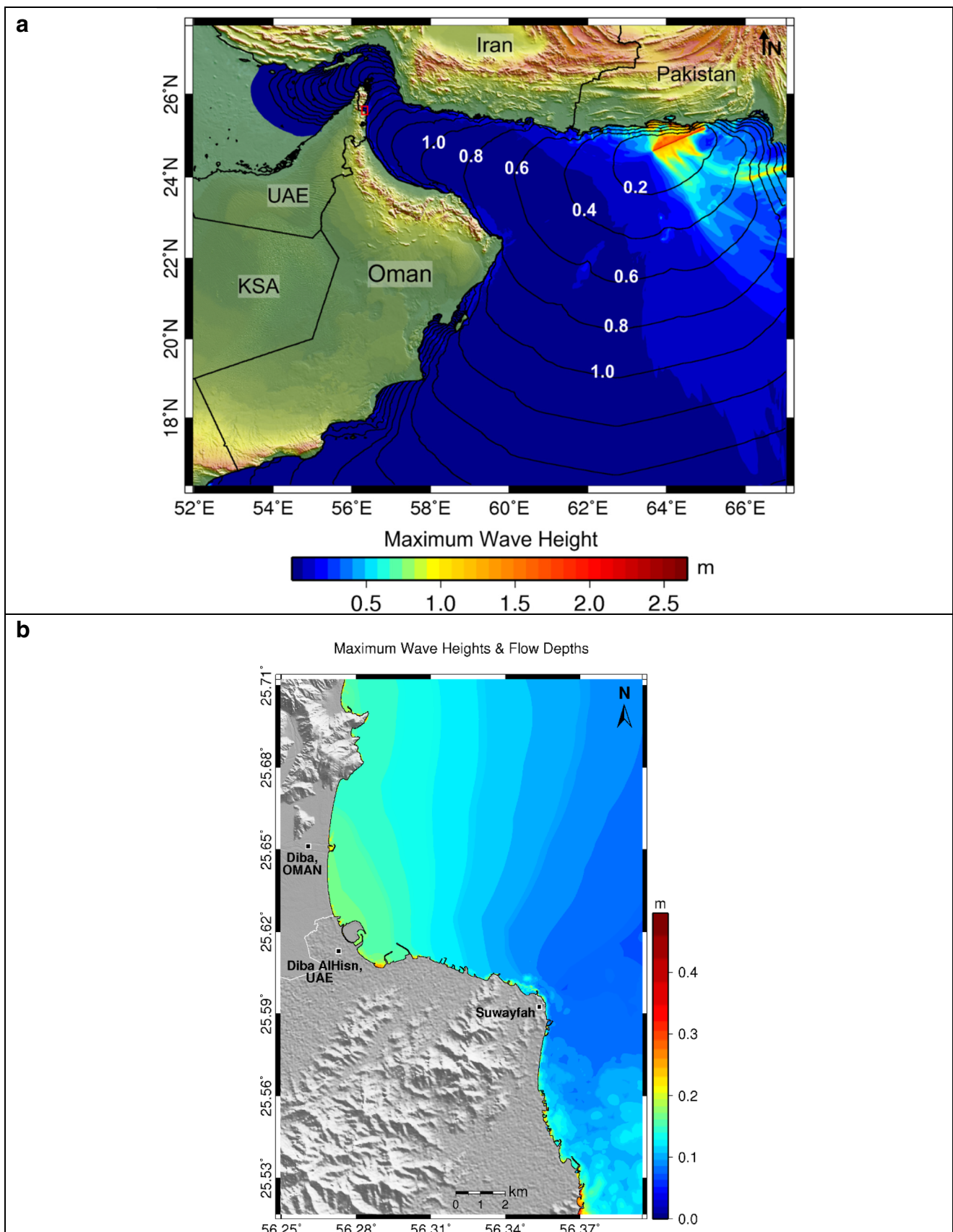


**Fig. 6** a Tsunami travel time in hours for the historic scenario 1945 earthquake, Mw 8.1, b tsunami hazard map for Diba representing maximum wave height and inundation in meters for scenario of 1945 earthquake, Mw 8.1

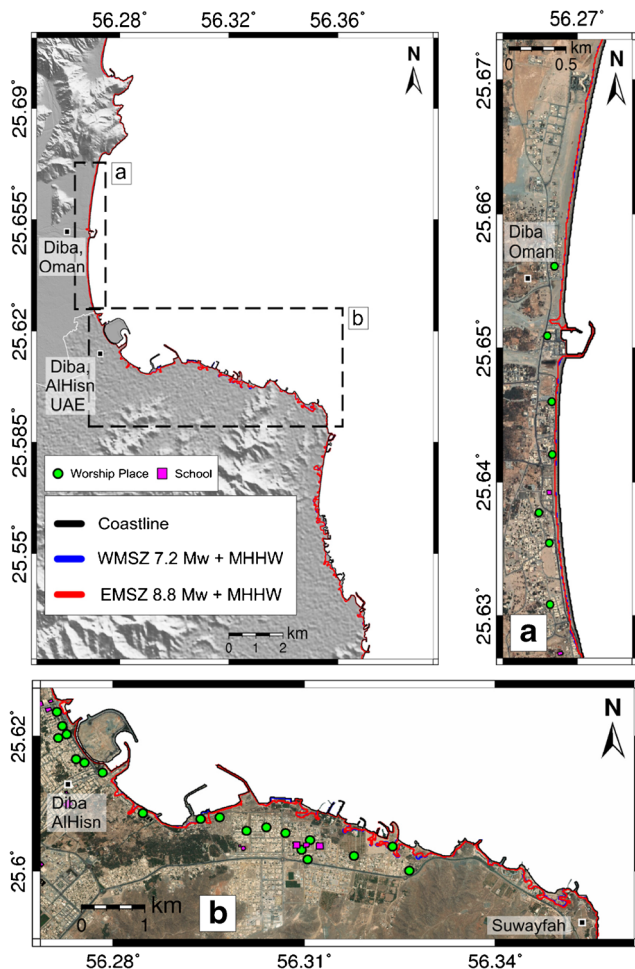


**Fig. 7** Inundation area for the worst-case scenarios for EMSZ and WMSZ for Mean Higher High water (MHHW) tidal condition

### Probabilistic tsunami hazard

PTHA along Diba coast concerns the determination of the probability that maximum tsunami wave heights/flow depths of 0.05, 0.25, 0.5, and 1.0 m are exceeded during given exposure times of 100 and 500 years.

Figure 8 depicts the exceedance likelihood of a maximum tsunami wave height/flow depth of 0.05 m (Fig. 8a), 0.25 m (Fig. 8b), 0.5 m (Fig. 8c), and 1.0 m (Fig. 8d) along the coast of Diba for an exposure time of 100 years. The 100-year PTHA results clearly show that MSZ earthquakes pose an overall low-to-moderate tsunami hazard on the Diba coast. Here, although the probability that a maximum tsunami wave height/flow depth exceeds 0.05 m is high (90–100%, Fig. 8a), it significantly decreases to 40–80% for the threshold of 0.25 m (Fig. 8b), to 10–40% for the threshold of 0.5 m (Fig. 8c), and to 0–10% for the threshold of 1.0 m (Fig. 8d).

As expected, the tsunami hazard on Diba coast increases with the increase of the average return period (i.e., 500-year in Fig. 9). The 500-year PTHA maps show probability of exceedance of 100% along the entire coast of Diba for 0.05 m

wave height (Fig. 9a). This probability ranges from 70 to 100% and from 30 to 80% for maximum wave height thresholds of 0.25 m and 0.5 m, respectively (Fig. 9b and c). This probability ranges from 0 to 10% for maximum wave height thresholds of 1.0 m (Fig. 9d).

## Discussion

### Methodology limitations

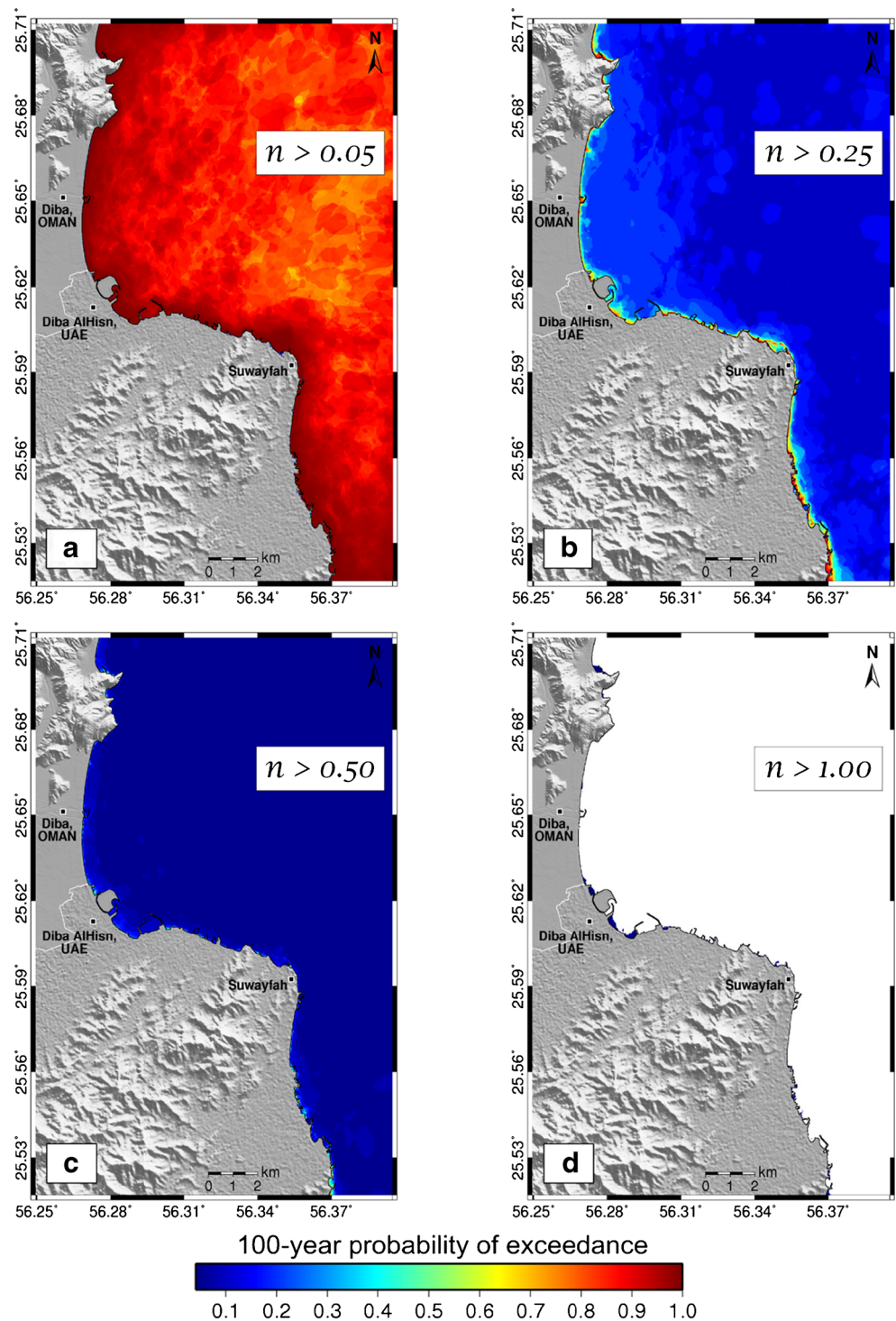
This study uses the state-of-the-art method for the DTHA and a logic-tree method for the PTHA for specific coastal sites of the Oman Sea. Both methodologies adopted here have the advantage of being easily applicable to any coastal area whenever high-resolution DEM is available. However, DTHA can suffer important limitations due to its sensitivity to selection of the source scenario (Geist and Lynett 2014). Therefore, in our study, it is worth mentioning that the DTHA results for Diba have inherent limitations coming from the geological unknowns and uncertainties on earthquake source parameters, in addition to others from the quality of the baseline data.

PTHA, on the other hand, includes treatment of uncertainty. In general, there are two categories of PTHA uncertainties: aleatoric referring to the random nature of tsunami generation and its effects and epistemic related to the insufficient knowledge on data and modeling accuracy (Annaka et al. 2007). PTHA for Diba coasts considers only the aleatoric uncertainty on the source location by letting the earthquake rupture float along the fault trace to generate multiple scenarios. This approach is valid in regions where the tsunamigenic source zone is well constrained (i.e., Makran subduction zone) (Omira et al. 2015). In complex seismogenic regions, other approaches such as the Monte Carlo are more suitable to treat the uncertainty on the source location (Geist and Parsons 2006). Epistemic uncertainties, such as those related to the tsunami modeling and accuracy of the DEM data, were not considered in the PTHA for Diba coasts. This fact presents an additional limitation of this study.

### Tsunami hazard on Diba coast

Tsunami hazard along the coasts of Diba-Oman and Diba-UAE can be considered moderate as shown by both DTHA and PTHA results of this study. It is mainly dominated by large earthquakes ( $M_w > 8.0$ ) occurring in the eastern MSZ. The geographical location of the study area, within the western coast on Oman Sea near the Hormuz Strait, also plays a protective role as most of tsunami energy from events on the eastern MSZ is steered towards Pakistan and the eastern coasts of Oman Sea. The threat posed by events of the closer western MSZ is comparable to the one from the farther eastern MSZ. This is because we consider that the eastern MSZ has the

**Fig. 8** 100-year PTHA on the coast of Diba. Probability that a maximum wave height/flow depth: **a** exceeds 0.05 m, **b** exceeds 0.25 m, **c** exceeds 0.5 m, and **d** exceeds 1.0 m along the coast of Diba for an exposure time of 100 years



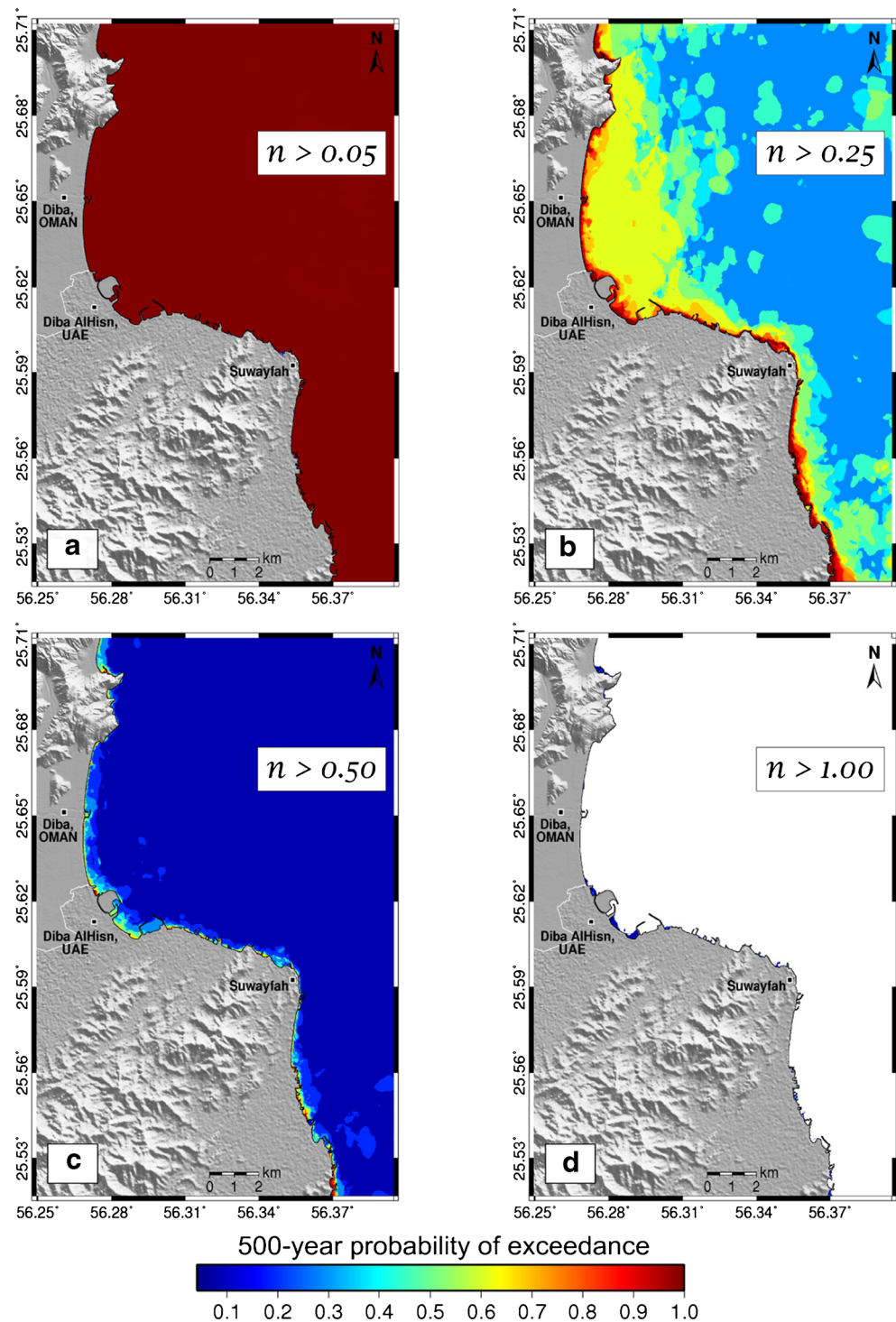
potential of generating a Mw 8.8 earthquake, while the worst-case scenario at the western MSZ has a Mw 7.2.

The PTHA results presented here expand and complement the previous work by El-Hussain et al. (2016) that evaluates the regional PTHA along the entire coast of Oman. Considering together the results of this study and those of El-Hussain et al. (2016), the northern coast of Oman, where

Diba is located, is less hazardous than the northeastern coasts (Muscat and Sur).

The comparison of DTHA and PTHA results evidences that the deterministic analysis leads to higher tsunami impact at Diba coasts. This difference can result from considering for DTHA the largest possible earthquake to occur without considering its recurrence interval as for PTHA. In addition, the

**Fig. 9** 500-year PTHA on the coast of Diba. Probability that a maximum wave height/flow depth: **a** exceeds 0.05 m, **b** exceeds 0.25 m, **c** exceeds 0.5 m, and **d** exceeds 1.0 m along the coast of Diba for an exposure time of 500 years



MHHW tidal condition is considered in the DTHA, while uncertainty on tidal stage is not treated in the PTHA. Despite this limitation in our PTHA, the conducted probabilistic analysis remains more complete as it takes in consideration the contribution of large and small possible events. For delimitation of evacuation zones, the scenario MHHW should be considered.

## Conclusions

Tsunami hazard on Diba coasts is evaluated using both deterministic and probabilistic methods. The study focusses on near-field tsunamigenic potential from the earthquakes generated at the MSZ. Both DTHA and PTHA are performed using a benchmarked shallow water numerical code and a high-

resolution digital elevation model of a 30-km long coastal area of Oman Sea hosting Diba-Oman and Diba-UAE. DTHA results are presented in terms of maximum wave heights and inundation maps for two worst-case scenarios and one historic case scenario. PTHA results express 100- and 500-year exposure times exceedance probabilities for the hazard intensities (i.e., wave height and flow depth) of 0.05, 0.25, 0.5, and 1.0 m. The main findings of this study are:

1. The worst-case scenario (Mw8.8 earthquake in the eastern MSZ with MHHW condition) causes a maximum flow depth of 1.90 m and a runup height of 2.80 m at Diba coasts.
2. The worst-case scenario from the western MSZ (Mw7.2 earthquake with MHHW condition) generates lower impact on Diba coast, with tsunami runup height in the range of 2.3 m.
3. The 1945 historical scenario produces insignificant tsunami impact on Diba coasts, with runup height of 0.2m.
4. In 100 years, exposure time, the probability that a maximum wave height/flow depth exceeds 0.5 m along the coasts of Diba ranges from 10 to 40%.
5. For an average return period of 500 years, the likelihood that a maximum wave height/flow depth exceeds 0.5 m along the coasts of Diba ranges from 30 to 80%.

**Funding** This study was funded by Sultan Qaboos University in joint grant with UAE University (project CL/SQU-UAEU/16/06). The authors appreciate the Earthquake Monitoring Center computing facilities. The authors acknowledge the FCT-Portugal (Fundação para a Ciência e Tecnologia) support through the project UIDB/50019/2020 – IDL.

## Declarations

**Conflict of interest** The author(s) declare that they have no competing interests.

## References

- Annaka T, Satake K, Sakakiyama T, Yanagisawa K, Shuto N (2007) Logic-tree approach for probabilistic tsunami hazard analysis and its applications to the Japanese coasts. *Pure Appl Geophys* 164:577–592. <https://doi.org/10.1007/s00024-006-0174-3>
- Baptista MA, Omira R, Miranda JM, El Hussain I, Deif A, Habsi ZA (2014) On the source of the 24 September 2013 tsunami in Oman Sea. *EGUGA*, 6185
- Baptista MA, Miranda JM, Matias L, Omira R (2017) Synthetic tsunami waveform catalogs with kinematic constraints. *Nat Hazards Earth Syst Sci* 17:1253–1265
- Baptista MA, Miranda JM, Omira R, El-Hussain I (2020) Study of the 24 September 2013 Oman Sea tsunami using linear shallow water inversion. *Arab J Geosci* 13(14):1–12
- Bayer R, Chery J, Tatar M, Vernant P, Abbassi M, Masson F, Bellier O (2006) Active deformation in Zagros—Makran transition zone inferred from GPS measurements. *Geophys J Int* 165(1):373–381
- Byrne DE, Sykes LR, Davis SM (1992) Great thrust earthquakes and aseismic slip along the plate boundary of the Makran Subduction Zone. *J Geophys Res* 97:449–478
- Deif A, El Hussain I (2012) Seismic moment rate and earthquake mean recurrence interval in the major tectonic boundaries around Oman. *J Geophys Eng* 9:773–783. <https://doi.org/10.1088/1742-2132/9/6/773>
- Deif A, El-Hussain I, Alshijbi Y, Mohamed AME (2020) Updating a probabilistic seismic hazard model for Sultanate of Oman. *Arab J Geosci* 13(13):1–21. <https://doi.org/10.1007/s12517-020-05394-8>
- El-Hussain I, Omira R, Deif A, Al-Habsi Z, Al-Rawas G, Mohamad A, Al-Jabri K, Baptista MA (2016) Probabilistic tsunami hazard assessment along Oman coast from submarine earthquakes in the Makran subduction zone. *Arab J Geosci* 9:888, 1–14. <https://doi.org/10.1007/s12517-016-2687-0>
- El-Hussain I, Omira R, Al-Bloushi K, Deif A, Al-Habsi Z, Al-Rawas G, Mohamed, AME, Al-Jabri K, Baptista MA (2017) Tsunami hazard assessment along Diba-Oman and Diba-Al-Emirates coasts, MATEC Web of Conferences 120, 06007 (2017) 71200. <https://doi.org/10.1051/mateconf/201712006007>
- El-Hussain I, Omira R, Al-Habsi Z, Baptista MA, Deif A, Mohamed AME (2018) Probabilistic and deterministic estimates of near-field tsunami hazards in northeast Oman. *Geosci Lett* 5. <https://doi.org/10.1186/s40562-018-0129-4>
- Geist EL, Lynett PJ (2014) Source processes for the probabilistic assessment of tsunami hazards. Special Issue on Undersea Natural Hazards, *Oceanography* 27(2):86–93. <https://doi.org/10.5670/oceanog.2014.43>
- Geist E, Parsons T (2006) Probabilistic analysis of tsunami hazards. *Nat Hazards* 37:277–314. <https://doi.org/10.1007/s11069-005-4646-z>
- Grezio A, Babeyko A, Baptista MA, Behrens J, Costa A, Davies G, Geist EL, Glimsdal S, González FI, Griffin J, Harbitz CB, LeVeque RJ, Lorito S, Løvholt F, Omira R, Mueller C, Paris R, Parsons T, Polet J, Power W, Selva J, Sørensen MB, Thio HK (2017) Probabilistic tsunami hazard analysis: multiple sources and global applications. *Rev Geophys* 55:1158–1198. <https://doi.org/10.1002/2017RG000579>
- Kukowski N, Schillhorn T, Flueh ER, Huhn K (2000) Newly identified strike-slip plate boundary in the northeastern Arabian Sea. *Geology* 28(4):355–358
- Minshull TA, White RS, Barton PJ, Collier JS (1992) Deformation at plate boundaries around the Gulf of Oman. *Mar Geol* 104(1–4): 265–277
- Miranda JM, Luis J, Reis C, Omira R, Baptista MA (2014) Validation of NSWING, a multi-core finite difference code for tsunami propagation and run-up. American Geophysical Union (AGU) Fall Meeting, San Francisco. Paper Number: S21A-4390. Session Number and Title: S21A, Natural Hazards
- Mokhtari M, Fard IA, Hessami K (2008) Structural elements of the Makran region, Oman Sea and their potential relevance to tsunamigenesis. *Nat Hazards* 47(2):185–199
- Molnar P (1979) Earthquake recurrence intervals and plate tectonics. *Bull Seismol Soc Am* 69:115–133
- Musson RMW (2009) Subduction in the Western Makran: the historian's contribution. *J Geol Soc* 166(3):387–391
- Okada Y (1985) Surface deformation due to shear and tensile faults in a halfspace. *Bull Seismol Soc Am* 75(4):1135–1154
- Okal EA, Fritz HM, Raad PE, Synolakis C, Al-Shijbi Y, Al-Saifi M (2006) Oman field survey after the December 2004 Indian Ocean Tsunami. *Earthquake Spectra* 22(S3):203–218
- Omira R, Baptista MA, Matias L (2015) Probabilistic tsunami hazard in the northeast atlantic from near-and far-field tectonic sources. *Pure Appl Geophys* 172(3–4):901–920. <https://doi.org/10.1007/s00024-014-0949-x>
- Omira R, Matias L, Baptista MA (2016a) Developing an event-tree probabilistic tsunami inundation model for NE Atlantic coasts:

- application to a case study. *Pure Appl Geophys* 173(12):3775–3794. <https://doi.org/10.1007/s00024-016-1367-z>
- Omira R, Baptista MA, Lisboa F (2016b) Tsunami characteristics along the Peru–Chile trench: analysis of the 2015 Mw8.3 Illapel, the 2014 Mw8.2 Iquique and the 2010 Mw8.8 Maule Tsunamis in the Near-field. *Pure Appl Geophys* 173(4):1063–1077. <https://doi.org/10.1007/s00024-016-1277-0>
- Pararas-Carayannis G (2006) The potential of tsunami generation along the Makran Subduction Zone in the northern Arabian Sea: case study: the earthquake and tsunami of November 28, 1945. *Sci Tsunami Hazards* 24(5):358–384
- Pendse CG (1946) The Mekran earthquake of the 28th November 1945. *Sci Notes* 10:141–145
- Rashidi A, Dutykh D, Shomali ZH, Keshavarz Farajkhah N, Nouri M (2020a) A Review of tsunami hazards in the Makran Subduction Zone. *Geosciences* 10:372. <https://doi.org/10.3390/geosciences10090372>
- Rashidi A, Shomali ZH, Dutykh D, Keshavarz Farajkhah N (2020b) Tsunami hazard assessment in the Makran subduction zone. *Nat Hazards* 100(2):861–875
- Titov V, Rabinovich AB, Moffeld HO, Thomson RE, Gonzalez FI (2005) The global reach of the 26 December 2004 Sumatra tsunami. *Science* 309(5743):2045–2048
- Vernant P, Nilforoushan F, Hatzfeld D, Abassi MR, Vigny C, Masson F, Nankali H, Martinod J, Ashtiani A, Bayer R, Tavakoli F, Chery J (2004) Present-day crustal deformation and plate kinematics in Middle East constrained by GPS measurements in Iran and northern Oman. *Geophys J Int* 157:381–398
- Zarifi Z (2006) Unusual subduction zones: Case studies in Colombia and Iran PhD thesis University of Bergen, Norway